Chapter 2
Ultra Short and Intense Laser Pulses

In the following chapter fundamental aspects of laser pulses and their interaction with single electrons will be discussed. At first the mathematical description of laser pulses is given. The relation between time and frequency domain will be explained and the concept of generating ultra short pulses will be sketched shortly. Then the interaction of the laser pulse with single electrons in the relativistic case will be discussed and the ponderomotive force will be introduced.

2.1 Mathematical Description

The electric field of short laser pulses can be described either in the time or the frequency domain. Both formalisms are related to each other by the Fourier transformation:

$$E(t) = \frac{1}{\sqrt{2\pi}} \int_{-\infty}^{\infty} \tilde{E}(\omega)\, e^{i\omega t}\, d\omega, \tag{2.1}$$

$$\tilde{E}(\omega) = \frac{1}{\sqrt{2\pi}} \int_{-\infty}^{\infty} E(t) e^{-i\omega t}\, dt. \tag{2.2}$$

Due to the fact that $E(t)$ is real, the symmetry of $\tilde{E}(\omega)$ is given as follows:

$$\tilde{E}(\omega) = \tilde{E}^{*}(-\omega), \tag{2.3}$$

where (*) indicates the complex conjugated function. The symmetry shows that the whole information of the pulse is already given in the positive part of the function. Thus, the reduced function $\tilde{E^{+}}(\omega)$ is defined as:

T. Sokollik, *Investigations of Field Dynamics in Laser Plasmas with Proton Imaging,* Springer Theses, DOI: 10.1007/978-3-642-15040-1_2,

$$\tilde{E^{+}}(\omega) = \begin{cases} \tilde{E}(\omega) & \text{if} \quad \omega \geq 0 \\ 0 & \text{if} \quad \omega < 0 \end{cases} \tag{2.4}$$

The inverse Fourier transformation of $\tilde{E^{+}}(\omega)$ delivers a description of the electric field which is a complex function now. Thus, both functions can be expressed by their amplitude and phase:

$$E^{+}(t) = A_{ampl}(t)\, e^{i\phi(t)}, \tag{2.5}$$

$$\tilde{E^{+}}(\omega) = \tilde{A}_{ampl}(\omega)\, e^{-i\tilde{\phi}(\omega)}. \tag{2.6}$$

The phase functions $\phi(t)$ and $\tilde{\phi}(\omega)$ can be developed by Taylor series:

$$\phi(t) = \sum_{j=0}^{\infty} \frac{a_j}{j!} t^j, \tag{2.7}$$

$$\tilde{\phi}(\omega) = \sum_{j=0}^{\infty} \frac{\tilde{a}_j}{j!} \omega^j. \tag{2.8}$$

The coefficients of the zeroth order $(a_0, \tilde{a_0})$ represent a constant phase, which shifts the carrier wave within the fixed envelope ("carrier-envelope phase"). The first order coefficients $(a_1, \tilde{a_1})$ shift the pulse in time and in frequency domain, respectively. With the slowly varying envelope approximation (SVEA) [1] a residual phase can be defined where ω_L represents the central laser (angular) frequency:

$$\varphi(t) = \phi(t) - \omega_L t. \tag{2.9}$$

The time dependent instantaneous (angular) frequency can be defined by:

$$\omega(t) = \frac{d\phi(t)}{dt} = \omega_L + \frac{d\varphi(t)}{dt}. \tag{2.10}$$

If the instantaneous frequency is constant in time the pulse is called unchirped and represents a bandwidth-limited pulse, the shortest pulse which can be created with a given spectral width. Pulse duration τ_L and spectral bandwidth $\Delta\omega_p$ are connected by:

$$\tau_L \Delta\omega_L \geq c_B, \tag{2.11}$$

due to the Fourier transformation (Eqs. 2.1 and 2.2). The constant c_B depends on the spectral shape of the pulse (e.g. gaussian: $c_B = 4\ln 2$).

Higher ($j \geq 1$) orders of the spectral phase are often not temporally constant. That means that the instantaneous frequency is changing in time. If the frequency increases/decreases the pulse is called up-/down-chirped.[1] A pulse with $d\omega(t)/dt = d^2\varphi(t)/dt^2 = a_2 = const$ is called linearly chirped, the frequency is changing

[1] Alternative notation: positive-/negative-chirped.

linearly in time. Pulses gain higher orders of the spectral phase, e.g. by dispersion, when propagating through material. In the Chirped Pulse Amplification (CPA) [2] scheme a linear chirp is generated by different propagation distances of the spectral components. The stretched pulse is amplified without the risk of damaging the optical components (especially the amplifier crystals). After amplification the chirp is compensated by a compressor consisting of two gratings mostly. Alternative schemes exist to compensate higher orders (≥ 1), for example chirped mirrors [3], prisms or a deformable mirror in the compressor to vary the propagation length of the spectral components.

Aside from generating bandwidth-limited pulses by flattening the spectral phase a defined manipulation of the spectral components by a "pulse shaper" (e.g. a liquid-crystal display in the spectral split beam) leads to special temporally shaped pulses which are of interest for several applications [4, 5].

Assuming a constant phase the pulse duration is limited by the spectral bandwidth. To shorten the pulse duration further the bandwidth has to be increased. For this, different methods can be used e.g. self-phase modulation (SPM) in gas-filled hollow fibers [6], or the generation of pulse filaments in gas-filled tubes [7]. The use of these techniques is limited to several mJ pulse energy. Self-phase modulation affects the phase and broadens the bandwidth without influencing the temporal amplitude. Thus, an additional pulse compression is necessary. Recent experiments at the Max-Born-Institute showed that under some conditions the pulse can be self-compressed by pulse filamentation [8, 9]. Details concerning these experiments, including measurements with the MBI TW laser can be found in reference [9].

Using Eqs. 2.5 and 2.9 the electric field can be split into the complex envelope function $A_{ampl}(t)\, e^{i\varphi(t)}$ and the fast oscillating term $e^{i\omega_L t}$:

$$E^{+}(t) = A_{ampl}(t)\, e^{i\varphi(t)} \cdot e^{i\omega_L t}. \tag{2.12}$$

The real valued temporal electric field can be now reconstructed from $E^{+}(t)$ as follows:

$$E(t) = 2Re(E^{+}(t)) \tag{2.13}$$

$$E(t) = 2A_{ampl}(t)\cos(\omega_L t + \varphi(t)). \tag{2.14}$$

Averaging the electric field, the temporal intensity can be calculated:

$$I(t) = \varepsilon_0 c \frac{1}{T} \int_{t-T/2}^{t+T/2} E^2(t')\, dt'. \tag{2.15}$$

If the slowly varying envelope approximation is valid Eq. 2.15 can be reduced to:

$$I(t) = 2\varepsilon_0 c A_{ampl}^2(t). \tag{2.16}$$

This formula defines the temporal intensity for a linear polarized laser pulse. In the experiments the peak intensity is usually used to characterize the laser pulses:

$$I_0 = \frac{1}{2}\varepsilon_0 c E_0^2 \tag{2.17}$$

and is typically given in [W/cm^2].

2.2 Single Electron Interaction

The motion of an electron caused by an electromagnetic field $\boldsymbol{E}$ and $\boldsymbol{B}$ in vacuum is described by the Lorentz equation [1]:

$$\frac{d\boldsymbol{p}}{dt} = \frac{d\,(\gamma m_e \boldsymbol{v})}{dt} = -e(\boldsymbol{E} + \boldsymbol{v} \times \boldsymbol{B}). \tag{2.18}$$

In the non-relativistic regime ($\gamma = 1/\sqrt{1 - v^2/c^2} \approx 1$) the electron oscillates in a linearly polarized laser field with an amplitude (y_0) and a maximum velocity (v_0) of:

$$y_0 \approx \frac{e\,E_0}{m_e\,\omega_L^2}, \qquad v_0 \approx \frac{e\,E_0}{m_e\,\omega_L}, \tag{2.19}$$

assuming a plane wave ($E_0 = 2\ A_{ampl}$) with the (angular) frequency ω_L. The maximum velocity is used to define the dimensionless normalized vector potential a_0:

$$a_0 = \frac{v_0}{c} = \frac{e\,E_0}{m_e\,\omega_L\,c}. \tag{2.20}$$

Using Eqs. 2.17 and 2.20 the laser intensity is given by:

$$I_0 = \frac{a_0^2}{\lambda^2} \cdot \frac{\varepsilon_0 m_e^2 c^5}{2e^2} (2\pi)^2 \approx \frac{a_0^2}{\lambda^2} \cdot 1.37 \cdot 10^{18}\,\mathrm{W/cm^2} \cdot \mu\mathrm{m}^2. \tag{2.21}$$

To calculate the electron trajectories for $a_0 \geq 1$, the equation of motion (Eq. 2.18) has to be discussed fully relativistically. This corresponds to an intensity of $>10^{18}$ W/cm^2. Assuming a linearly polarized plane wave propagating in the x-direction with the vector potential $\boldsymbol{A}$:

$$\boldsymbol{A} = (0, A_0\,\sin{(k\,x - \omega_L\,t)}, 0), \tag{2.22}$$

the electric and magnetic field can be described as follows:

$$\boldsymbol{E} = -\frac{\partial \boldsymbol{A}}{\partial t} = E_0 \cos{(k\,x - \omega_L t)}\,\boldsymbol{e_y}, \quad E_0 = \omega_L A_0 \tag{2.23}$$

$$\boldsymbol{B} = \nabla \times \boldsymbol{A} = B_0 \cos(kx - \omega_L t)\, \boldsymbol{e}_z, \qquad B_0 = kA_0. \tag{2.24}$$

Substituting Eq. 2.18 with these formulas the equation of motion can be written as:

$$\frac{d\boldsymbol{p}}{dt} = e\left(\frac{\partial \boldsymbol{A}}{\partial t} - \boldsymbol{v} \times (\nabla \times \boldsymbol{A})\right). \tag{2.25}$$

The momentum in y-direction is determined by:

$$\frac{dp_y}{dt} = e\left(\frac{\partial A_y}{\partial t} + v_x \frac{\partial A_y}{\partial x}\right) \tag{2.26}$$

$$p_y - eA_y = \alpha_1. \tag{2.27}$$

The constant α_1 is related to the initial momentum in y-direction. Since the magnetic field has a component in z-direction only, the momentum in x-direction is determined by (cf. Eq. 2.18):

$$\frac{dp_x}{dt} = -ev_y B_z = m_e c \frac{d\gamma}{dt}. \tag{2.28}$$

Using the energy equation and the relation between E_0 and B_0 from Eqs. 2.23 and 2.24:

$$\frac{d}{dt}(\gamma m_e c^2) = -e(\boldsymbol{v} \cdot \boldsymbol{E}), \tag{2.29}$$

$$\frac{E_0}{c} = B_0, \tag{2.30}$$

a description of the momentum in x-direction can be found:

$$\gamma - \frac{p_x}{m_e c} = \alpha_2, \tag{2.31}$$

where α_2 is the second invariant of the electron motion. Using $\gamma^2 = 1 + p^2/(m_e\, c)^2$ a relation between p_x and p_y is given by:

$$\gamma^2 = 1 + \frac{p_x^2}{(m_e c)^2} + \frac{p_y^2}{(m_e c)^2}, \tag{2.32}$$

$$\frac{p_x}{m_e c} = \frac{1 - \alpha_2^2 + (p_y/m_e c)^2}{2\alpha_2}. \tag{2.33}$$

To calculate the electron trajectories the following formula has to be integrated using $\boldsymbol{r} = (x, y, z)$:

$$\boldsymbol{p} = \gamma m_e \frac{d\boldsymbol{r}}{dt} = \gamma m_e \frac{d\boldsymbol{r}}{d\phi}\frac{d\phi}{dt} = -m_e \omega_L \frac{d\boldsymbol{r}}{d\phi}. \tag{2.34}$$

In case of a linearly polarized plane wave in y-direction the trajectories are determined with the initial values $t = 0$, $p_y = 0$, $x = 0$ and $y = 0$ ($\alpha_1 = 0$ and $\alpha_2 = 1$) by:

$$x = \frac{c\, a_0^2}{4\, \omega_L} \left(\phi - \frac{1}{2} \sin(2\phi) \right), \tag{2.35}$$

$$y = \frac{c\, a_0}{\omega_L} (1 - \cos \phi). \tag{2.36}$$

The y-coordinate is oscillating as in the non-relativistic regime, whereas the x-coordinate is oscillating with twice the laser frequency and with an additionally drift. The drift velocity v_D can be estimated averaging over one laser cycle:

$$\bar{x} = \frac{c\, a_0^2}{4\, \omega_L} \phi = \frac{c\, a_0^2}{4\, \omega_L} \omega_L\, t - \frac{c\, a_0^2}{4\, \omega_L} \frac{\omega_L}{c} \bar{x} \tag{2.37}$$

$$\bar{x} = \frac{c\, a_0^2}{4} t - \frac{a_0^2}{4} \bar{x} \tag{2.38}$$

$$v_D = \frac{\bar{x}}{t} = \frac{c\, a_0^2}{4 + a_0^2}. \tag{2.39}$$

In Fig. 2.1a, the trajectory of an electron is shown being in rest before hit by a plane wave with infinite duration. In a more realistic case when the electron is deflected by a laser pulse of finite duration, the electron is at rest after the electric field disappears. Thus, the particle does not gain net energy. The electron trajectory is shown in Fig. 2.1b–d for this case. The electron is pushed in laser forward direction while oscillating with the laser frequency and is at rest after the laser pulse is gone. In fact, this case is not realistic at all since the laser pulse is usually focused tightly. If the focus is in the range of the lateral deflection the electron can escape due to the decreasing intensity and thus due to the decreasing restoring force. The electron leaves at an angle θ dependent on its kinetic energy. This phenomenon is called ponderomotive scattering and will be discussed in the next section.

2.3 Ponderomotive Force

Averaging over the equation of motion in time leads to the definition of the ponderomotive force. This force is caused by the gradient of laser intensity which becomes relevant if e.g. a focused laser pulse or a density profile is present. In the following the ponderomotive force in vacuum will be discussed.

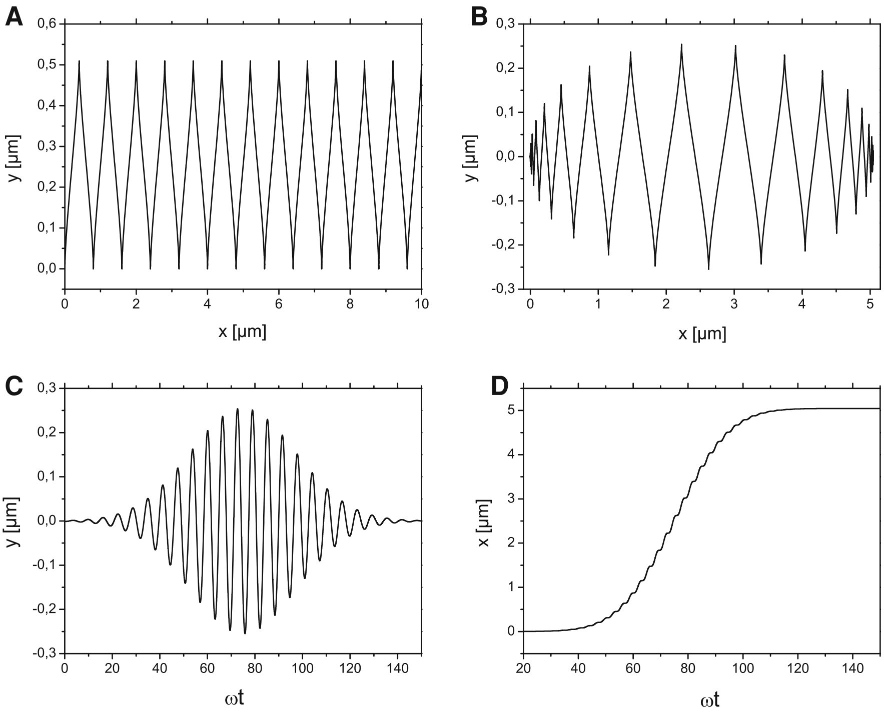

Fig. 2.1 **a** Electron trajectory caused by a infinite plane wave ($a_0 = 2$) (laboratory frame). **b–d** Electron trajectories for a pulse duration of 15 fs with same maximum intensity

In the non-relativistic case ($v/c \ll 1$) the equation of motion can be written as:

$$\frac{\partial v_y}{\partial t} = -\frac{e}{m_e} E_y(r). \tag{2.40}$$

The electric field E_y, polarized in y-direction and propagating in x-direction, has a radial intensity dependence[2] and can be expressed by a Taylor expansion as follows [1]:

$$E_y(r) \simeq E_0(y)\cos\phi + y\frac{\partial E_0(y)}{\partial y}\cos\phi + \cdots \tag{2.41}$$

where $\phi = \omega t - k\,x$. The first order can be calculated by integrating Eq. 2.40 using Eq. 2.41:

$$v_y^{(1)} = -\frac{eE_0}{m_e\omega}\sin\phi, \qquad y^{(1)} = \frac{eE_0}{m_e\omega^2}\cos\phi. \tag{2.42}$$

[2] Only the dependence in the y-direction will by considered in the following.

Using Eqs. 2.42 and 2.40 one gets:

$$\frac{\partial v_y^{(2)}}{\partial t} = -\frac{e^2}{m_e^2\omega^2} E_0 \frac{\partial E_0(y)}{\partial y} \cos^2 \phi. \tag{2.43}$$

Averaging the corresponding force over one cycle leads to:

$$f_{pond} = \overline{m_e \frac{\partial v_y^{(2)}}{\partial t}} = -\frac{e^2}{4m_e\omega^2} \frac{\partial E_0^2(y)}{\partial y}. \tag{2.44}$$

This is the definition of the ponderomotive force in the non-relativistic case. Since the force is dependent on the gradient of E_0^2 electrons will be pushed away from regions of higher intensities. The fully relativistic discussion delivers an additional factor $(1/\langle\gamma\rangle)$ where $\langle\gamma\rangle$ is the relativistic factor γ averaged over the fast oscillations [10]:

$$f_{pond,rel} = -\frac{e^2}{4m_e\langle\gamma\rangle\omega^2} \frac{\partial E_0^2(y)}{\partial y}. \tag{2.45}$$

The angle between electron trajectory and the laser axis can be determined by the ratio of the transversal and longitudinal momentum:

$$\tan\theta = \frac{p_y}{p_x} = \sqrt{\frac{2}{\gamma - 1}}, \tag{2.46}$$

or

$$\cos\theta = \sqrt{\frac{\gamma - 1}{\gamma + 1}}. \tag{2.47}$$

For a linearly polarized and focused laser pulse one would expect an angular spread of the scattered electrons only in the x–y-plane (polarization plane). Due to the fact that for a focused laser pulse an axial magnetic field $B_x = \frac{\partial A_y}{\partial z}$ exists, a force in the z-direction of the same order as the y-component of the ponderomotive force will act. Thus, the electrons are scattered radially symmetrical [1, 11–14].

References

1. P. Gibbon, *Short Pulse Laser Interactions with Matter: An Introduction* (World Scientific Publishing Company, Singapore, 2005)
2. D. Strickland, G. Mourou, Compression of amplified chirped optical pulses. Opt. Commun. **56**(3), 219–221 (1985)
3. R. Szipocs, K. Ferencz, C. Spielmann, F. Krausz, Chirped multilayer coatings for broad-band dispersion control in femtosecond lasers. Opt. Lett. **19**(3), 201–203 (1994)

4. A. Assion, T. Baumert, M. Bergt, T. Brixner, B. Kiefer, V. Seyfried, M. Strehle, G. Gerber, Control of chemical reactions by feedbackoptimized phase-shaped femtosecond laser pulses. Science **282**(5390), 919–922 (1998)
5. T. Brixner, G. Krampert, T. Pfeifer, R. Selle, G. Gerber, M. Wollenhaupt, O. Graefe, C. Horn, D. Liese, T. Baumert, Quantum control by ultrafast polarization shaping. Phys. Rev. Lett. **92**(20), 208301 (2004)
6. M. Nisoli, S. De Silvestri, O. Svelto, Generation of high energy 10 fs pulses by a new pulse compression technique. Appl. Phys. Lett. **68**(20), 2793–2795 (1996)
7. A. Couairon, M. Franco, A. Mysyrowicz, J. Biegert, U. Keller, Pulse self-compression to the single-cycle limit by filamentation in a gas with a pressure gradient. Opt. Lett. **30**(19), 2657–2659 (2005)
8. G. Stibenz, N. Zhavoronkov, G. Steinmeyer, Self-compression of millijoule pulses to 7.8 fs duration in a white-light filament. Opt. Lett. **31**(2), 274–276 (2006)
9. S. Skupin, G. Stibenz, L. Berge, F. Lederer, T. Sokollik, M. Schnurer, N. Zhavoronkov, G. Steinmeyer, Self-compression by femtosecond pulse filamentation: Experiments versus numerical simulations. Phys. Rev. E **74**(5), 056604–9 (2006)
10. B. Quensel, P. Mora, Theory and simulation of the interaction of ultraintense laser pulses with electrons in vacuum. Phys. Rev. E **58**(3), 3719–3732 (1998)
11. G. Malka, J. Fuchs, F. Amiranoff, S.D. Baton, R. Gaillard, J.L. Miquel, H. Pepin, C. Rousseaux, G. Bonnaud, M. Busquet, L. Lours, Suprathermal electron generation and channel formation by an ultrarelativistic laser pulse in an underdense preformed plasma. Phys. Rev. Lett. **79**(11), 2053–2056 (1997)
12. E. Lefebvre, G. Malka, J.L. Miquel, Lefebvre, Malka, and Miquel Reply. Phys. Rev. Lett. **80**(6), 1352 (1998)
13. K.T. McDonald, Comment on “Experimental observation of electrons accelerated in vacuum to relativistic energies by a high-intensity laser”. Phys. Rev. Lett. **80**(6), 1350 (1998)
14. P. Mora, B. Quesnel, Comment on “Experimental Observation of Electrons Accelerated in Vacuum to Relativistic Energies by a High- Intensity Laser”. Phys.l Rev. Lett. **80**(6), 1351 (1998)

http://www.springer.com/978-3-642-15039-5

Investigations of Field Dynamics in Laser Plasmas with
Proton Imaging
Sokollik, Th.
2011, XIV, 126 p., Hardcover
ISBN: 978-3-642-15039-5